Theoretical Studies on Hydrogen Bonding, NMR Chemical Shifts and Electron Density Topography in α, *β* and *γ*-Cyclodextrin Conformers

Rahul V. Pinjari, Kaustubh A. Joshi, and Shridhar P. Gejji*

Department of Chemistry, University of Pune, Ganeshkhind 411007, Pune, India

Received: June 12, 2007; In Final Form: September 10, 2007

Hydrogen-bonded interactions in α-, *β*-, and *γ*-CD conformers are investigated from the molecular electron density topography and chemical shift in the nuclear magnetic resonance (NMR) spectra calculated by using the Gauge Invariant Atomic Orbital (GIAO) method within the framework of density functional theory. For the lowest-energy CD conformers in the gas phase, the $O_3-H\cdots O_2'$ hydrogen-bonding interactions are present. Calculated ^1H NMR chemical shifts (δ_H) correlate well with the hydrogen-bond distance as well as electron density at the bond critical point in the molecular electron density (MED) topography. The conformers of *β*- and *γ*-CD comprised of relatively strong secondary hydroxyl interactions are stabilized by solvation from polar solvents.

Introduction

Cyclodextrins (CD) are the cyclic oligosaccharides comprised of six (α-CD), seven (*β*-CD), or eight (*γ*-CD) D-glucoses condensed through an α(1→4) linkage. Their hydrophobic internal cavity and hydrophilic external surface offer high molecular recognition ability toward a variety of guest molecules from polar inorganic ions to nonpolar organic molecules.[1] Well-defined chemical structure, a multitude of potential sites for chemical modification, varying cavity dimension, low toxicity, low pharmacological activity, and protection of the guest from biodegradation and bioadaptability[2−4] are some of the attributes which facilitate their use in biochemistry and drug research. The α-, *β*-, and *γ*-CDs in aqueous solution are conducive to the formation of inclusion complexes which find applications in pharmaceutical science, catalysis, and as building blocks for supramolecular structures.[5−13] These inclusion complexes crystallize either in cage- or channel-type structures depending on whether the guest is ionic or molecular in nature. Crystal structure data have shown that intermolecular O−H···O and C−H···O interactions favor the macrocyclic conformation and subsequent inclusion of the guest molecules.[14] The binding affinity of a guest in these complexes is governed by cavity dimension, its relative orientation, and noncovalent interactions which refer to both dipole−dipole and hydrogen-bonded interactions. Fluorescence, UV−visible spectroscopy, and calorimetry experiments enable one to measure complexation energies. These techniques, however, provide only indirect and qualitative information about inclusion modes and geometries. Thus, structural characterization pertaining to relative orientation of a guest in the CD cavity is of particular significance for the understanding of supramolecular host−guest complexation. Encapsulation of a guest in the CD cavity has been widely studied through NMR experiments.[15] Thus, the observed chemical shifts have emerged as an alternative means to single-crystal diffraction data derived from either the X-ray or neutron diffraction experiments to obtain insights regarding orientation of a guest in the complex. These NMR experiments have shown that hydrogen-bonded interactions of secondary hydroxyl groups from the bottom rim render less flexibility to *β*-CD than to α- or *γ*-CD.[16−19] This partly accounts for the low solubility of *β*-CD in water. Lipkowitz[20] has obtained the energies of open and closed conformers employing the empirical force field calculations. Dobado et al.[21] have calculated the chemical shifts in a series of modified cyclodextrins functionalized at the primary hydroxyl group from the density functional calculations. The chemical shifts thus obtained agree well with the experimental data. Recently, the electronic structure of anhydrous *β*-CD conformers has been reported.[22−25] Thermodynamic parameters such as free energies of CD complexation and the ^1H NMR spectra[15] are affected significantly by solvation. The topography of scalar fields such as the molecular electrostatic potential has recently been explored to analyze the hydrogen-bonded interactions involving primary as well as secondary hydroxyl groups of α-, *β*-, and *γ*-CD.[22] In the present work, α-, *β*-, and *γ*-CD conformers with different relative orientations of primary hydroxyl groups and clockwise and anticlockwise hydrogen-bonding patterns from both top and bottom rims are considered. The present paper is aimed at gaining insights for the molecular-level understanding of hydrogen-bonded interactions and how they manifest themselves in the calculated NMR chemical shift. Pursuant to this, the following questions have been addressed in this work. (i) How do the hydrogen-bonding patterns influence the energetics of α-, *β*-, and *γ*-CD conformers? (ii) How do the hydrogen-bonded interactions vary with the increasing cavity size of the CD? (iii) Can the NMR shifts be correlated to hydrogen-bond patterns or the size of the CD cavity? The computational method used is outlined below.

Computational Method

Hartree−Fock geometry optimizations of the α-, *β*-, and *γ*-CD conformers possessing different hydrogen-bonded patterns were carried out employing the internally stored 3-21G basis set. The geometries thus obtained are further subjected to the optimization (with no symmetry constraints) using density functional calculations incorporating Becke's three-parameter exchange with Lee, Yang, and Parr's (B3LYP) correlation functional using the 6-31G(d) basis set.[26,27] Calculations are

* Corresponding author. Fax: +91-20-2569 1728. E-mail: spgejji@chem.unipune.ernet.in.

10.1021/jp074539w CCC: $37.00
Published on Web 12/04/2007

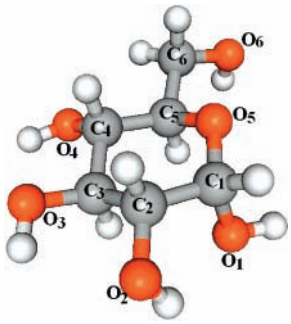

Figure 1. Glucose unit cut from cyclodextrin along with the atomic numbering scheme.

carried out using the GAUSSIAN 03 program.[28] The optimized geometry of a glucose residue cut out of CD is displayed in Figure 1. The atomic numbering scheme used is also shown along with the Figure. These optimized geometries should be regarded as the stationary point geometries on the potential energy surface since the vibrational frequency calculations for these CD conformers being computationally expensive for such large systems were not carried out in the present work. NMR chemical shifts (δ) were calculated by subtracting the nuclear magnetic shielding tensors of protons in CD from those of the tetramethyl silane (TMS) (as a reference) through the gauge invariant atomic orbital (GIAO) method[29] at the B3LYP/6-31G(d,p)//B3LYP/6-31G(d) level of theory. The Quantum Theory of Atoms in Molecules (QTAIM)[30−32] proposed by Bader was employed to investigate the molecular electron density topography and, accordingly, the bond critical point (bcp), characterized as (3,−1) CP, of different hydrogen bonds was located. A program developed in our laboratory was used to calculate the density at the bcp (ρ_{bcp}) in the MED topography.[33,34] The effect of solvation on the relative stabilization energies of these CD conformers was studied by using the self-consistent reaction field (SCRF) theory employing the Polarizable Continuum Model (PCM),[35] where the cavity is created via a series of overlapping spheres, initially devised by Tomasi and co-workers, as implemented in the GAUSSIAN 03 program.

Results and Discussion

For α-, β-, and γ-CD, conformers possessing primary as well as secondary hydroxyl groups oriented in clockwise and anticlockwise fashion are considered. These conformers are classified as "A", "B", and "C" by considering hydroxyl interactions from the primary OH groups. These conformers are displayed in Figure 2. Thus (i) conformers which have $O_6H\cdots O_6'$ interactions are referred as "A", (ii) those comprised of $O_6H\cdots O_5'$ interactions are denoted by "B", and (iii) those which have intra-glucose $O_6H\cdots O_5$ interactions (involving ether oxygens) are called "C". The single prime in these expressions refers to atoms from an adjacent glucose unit. We considered four conformers of "A" denoted by A1, A2, A3, and A4. Here, 1 refers to the hydroxyl protons oriented anticlockwise in the top rim and clockwise in the bottom; the conformer which has reverse orientations in top and bottom rims to the above is designated as 2. The labels 3 and 4 denote the hydroxyl groups oriented in top and bottom rims to be either both clockwise or both anticlockwise, respectively. With these notations only B3, B4, C1, and C2 conformers are possible. Accordingly, $O_2H\cdots O_3'$ interactions are present only in A2, A4, B2, and C4 conformers, whereas the A1, A3, B3, and C1 conformers facilitate $O_3H\cdots O_2'$ interactions. Relative stabilization energies of α-, β-, and γ-CD conformers from the B3LYP/6-31G(d) and B3LYP/6-31G(d,p)//B3LYP/6-31G(d) calculations are compared in Table 1. These stabilization energies were calculated by subtracting the electronic energy of the CD conformer from that of the corresponding lowest-energy conformer (A1) of α-, β-, and γ-CD. Calculated stabilization energies from both basis sets do not vary significantly. As may be noticed readily, the energies calculated using the 6-31G(d) basis set for the C1 conformer of β-CD differ maximally by 2.7 kJ mol^{-1} when the 2p polarization functions have been added on hydrogen atoms to the basis set. Further, the $O_6H\cdots O_6'$ interactions present only in the "A" type of conformers render stability to these conformers over "B" and "C" in a gas phase. Anticlockwise hydrogen bonding pattern in the top rim of CD is prevalent in the "A" type of conformers. It may further be noticed here that conformers comprised of $O_3H\cdots O_2'$ interactions are favored over those possessing the $O_2H\cdots O_3'$ interactions.

TABLE 1: Relative Stabilization Energies (ΔE in kJ mol^{-1}) of CD Conformers

	α-CD		β-CD		γ-CD	
	6-31G (d)	6-31G (d,p)[a]	6-31G (d)	6-31G (d,p)[a]	6-31G (d)	6-31G (d,p)[a]
A1	0.0	0.0	0.0	0.0	0.0	0.0
A2	1.9	−0.1	12.1	9.6	21.6	18.6
A3	2.3	0. 6	11.3	8.9	20.3	17.4
A4	−0.1	−0.4	0.6	0.3	0.3	0.1
B2	82.5	82.5	78.5	78.9	64.9	66.2
B3	76.8	77.5	75.3	76.5	64.2	66.2
C1	81.2	80.0	80.0	78.2	69.0	66.9
C4	88.0	85.8	84.7	82.0	72.2	69.4

[a] Energies are calculated at the B3LYP/6-31G(d,p)//B3LYP/6-31G(d) level of theory.

Selected hydrogen-bond distances involving primary (top rim) and secondary (bottom rim) hydroxyl groups of CD conformers are given in Table 2. As may be noticed, the inter-glucose $O_3H\cdots O_2'$ distances are predicted to be shorter in "C" as compared to those in the "B" or "A" types of conformers. Accordingly, for α-CD, the $O_3H\cdots O_2'$ hydrogen-bond distance in the lowest-energy conformers in "A", "B", and "C" turns out to be 2.156, 1.902, and 1.890 Å, respectively. Similar inferences may be drawn in the cases of β- and γ-CD. With an increase of cavity size from α-CD to γ-CD, the $O_3H\cdots O_2'$ and $O_2H\cdots O_3'$ interactions (from secondary hydroxyls) lead to shorter hydrogen-bond distances. These interactions are prevalent in "B" and "C" conformers relative to "A". The $O_6H\cdots O_6'$ interactions exhibit the trend α-CD > β-CD > γ-CD, which is parallel to the hydrogen-bond distances. For example, in A1 the $H\cdots O_6'$ distance turns out to be 1.798 Å in the case of α-CD compared to 1.890 Å for γ-CD. On the other hand, secondary hydroxyl groups exhibit a rank order opposite to that of primary hydroxyls as pointed out earlier.

The strength of hydrogen-bonded interactions can be gauged from the electron density at bcp (ρ_{bcp}) in the MED topography. The ρ_{bcp} values of hydrogen bonds in CD conformers are compared in Table 3. It may be inferred that the $O_6H\cdots O_6'$ (0.0350 au) interactions in α-CD are stronger than those in β-(0.0319 au) or γ-CD (0.0284 au). The hydrogen-bonded interactions at the bottom rim of "B" and "C" conformers are relatively stronger than those in conformer "A". An increase in ρ_{bcp} values from α- to β- to γ-CD for these interactions can thus be explained. The higher ρ_{bcp} observed for $O_3H\cdots O_2'$ hydrogen bonds as compared to $O_2H\cdots O_3'$ hydrogen-bonded interaction further support the energy rank order of CD conformers. The $O_3H\cdots O_2'$ interactions are, therefore, favored over $O_2H\cdots O_3'$ interactions in the lowest-energy conformers.

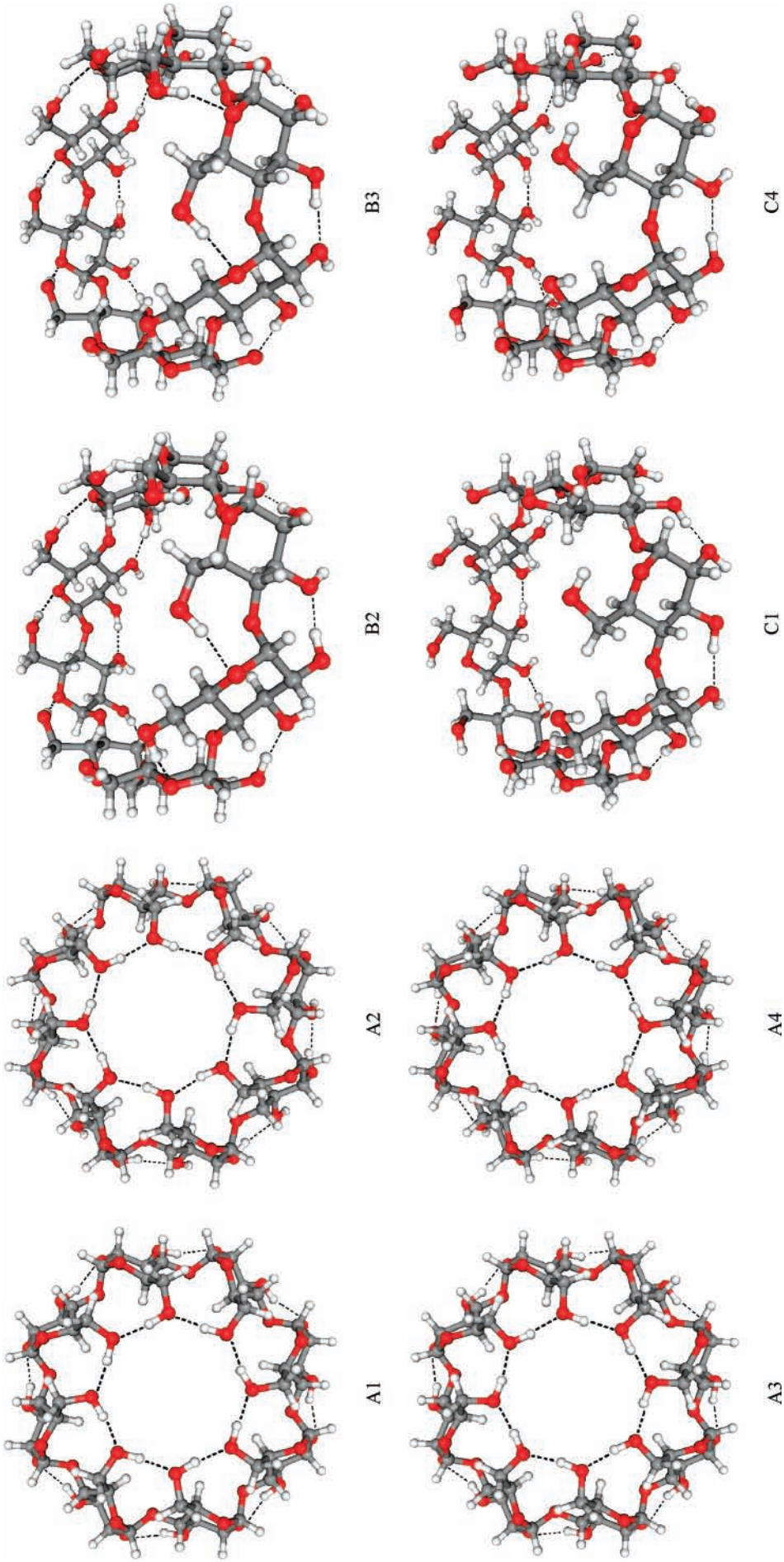

Figure 2. Clockwise and anticlockwise orientations of hydroxyl groups in the top and bottom rims of CD. These conformers are classified from the hydrogen-bonding pattern of primary hydroxyl groups. Conformers A having $O_6H\cdots O_6'$ interactions, conformers B having $O_6H\cdots O_5'$ interactions, and conformers C do not possess hydrogen-bonded interactions from primary hydroxyl groups.

TABLE 2: Selected Bond Distances (in Å) of α-, *β*-, and *γ*-CD Conformers[a]

	A1	A2	A3	A4	B2	B3	C1	C4
α-CD								
$O_2H\cdots O_3'$	(2.390)	2.238	2.390	2.182	1.895	(2.276)	(2.274)	1.901
$O_3H\cdots O_2'$	2.156	(2.422)	2.198	(2.429)	(2.320)	1.902	1.890	(2.326)
$O_6H\cdots O_6'$	1.798	1.808	1.810	1.797				
$O_6H\cdots O_5'$					1.943	1.949		
$C_6H\cdots O_5'$	2.447	2.288	2.335	2.406				
β-CD								
$O_2H\cdots O_3'$	(2.397)	2.185	(2.401)	2.146	1.875	(2.249)	(2.263)	1.906
$O_3H\cdots O_2'$	2.119	(2.423)	2.148	(2.430)	(2.286)	1.877	1.882	(2.308)
$O_6H\cdots O_6'$	1.838	1.850	1.846	1.833				
$O_6H\cdots O_5'$					1.925	1.928		
$C_6H\cdots O_5'$	2.411	2.265	2.309	2.369				
γ-CD								
$O_2H\cdots O_3'$	(2.415)	2.161	(2.413)	2.141	1.868	(2.233)	(2.255)	1.891
$O_3H\cdots O_2'$	2.101	(2.432)	2.129	(2.434)	(2.266)	1.864	1.862	(2.292)
$O_6H\cdots O_6'$	1.890	1.903	1.904	1.877				
$O_6H\cdots O_5'$					1.907	1.917		
$C_6H\cdots O_5'$	2.384	2.254	2.296	2.334				

[a] Figures in parenthesis indicate the intra-glucose O−H···O interactions from secondary hydroxyl groups at the bottom rim.

TABLE 3: Electron Density (ρ_{bcp}) at the bcp in MED Topography of α-, *β*-, and *γ*-CD Conformers

	conformers	A1	A2	A3	A4	B2	B3	C1	C4
$O_2H\cdots O_3'$	α-CD		0.0138		0.0156	0.0284			0.0281
	β-CD		0.0153		0.0167	0.0294			0.0276
	γ-CD		0.0160		0.0168	0.0296			0.0283
$O_3H\cdots O_2'$	α-CD	0.0163		0.0149			0.0282	0.0289	
	β-CD	0.0175		0.0164			0.0296	0.0293	
	γ-CD	0.0180		0.0169			0.0304	0.0305	
$O_6H\cdots O_6'$	α-CD	0.0350	0.0346	0.0345	0.0351				
	β-CD	0.0319	0.0313	0.0317	0.0322				
	γ-CD	0.0284	0.0279	0.0278	0.0286				
$O_6H\cdots O_5'$	α-CD					0.0275	0.0272		
	β-CD					0.0285	0.0283		
	γ-CD					0.0295	0.0289		
$C_6H\cdots O_5'$	α-CD	0.0114	0.0156	0.0142	0.0124				
	β-CD	0.0122	0.0163	0.0149	0.0133				
	γ-CD	0.0129	0.0166	0.0153	0.0143				

TABLE 4: ^{1}H NMR Chemical Shifts in Different α-, *β*-, and *γ*-CD Conformers

	conformers	A1	A2	A3	A4	B2	B3	C1	C4
O_2H	α-CD	2.05	2.77	2.03	2.97	4.31	2.58	2.52	4.24
	β-CD	2.05	3.02	2.02	3.18	4.49	2.65	2.56	4.20
	γ-CD	2.02	3.16	1.98	3.25	4.55	2.72	2.59	4.31
O_3H	α-CD	3.80	2.07	3.64	2.08	2.56	5.08	5.10	2.53
	β-CD	4.00	2.11	3.89	2.12	2.70	5.30	5.19	2.58
	γ-CD	4.13	2.12	3.98	2.13	2.77	5.45	5.38	2.65
O_6H	α-CD	5.57	5.91	5.88	5.58	2.90	2.85	1.28	1.28
	β-CD	5.12	5.49	5.52	5.19	3.02	2.98	1.25	1.26
	γ-CD	4.63	5.02	5.02	4.68	3.14	3.06	1.23	1.22

In the following we discuss how the hydrogen-bonding features influence the chemical shifts in NMR spectra. Hydrogen-bonded interactions lead to deshielding of the proton and hence a downshift for OH protons in the NMR spectra. Strength of the hydrogen bond can, therefore, be correlated to δ_H. Calculated δ_H values of the hydroxyl protons are reported in Table 4. It may readily be noticed that the O_6H proton exhibits a larger downshift. A plot of the $O_6H\cdots O_6'$ bond distance vs δ_H values of α-, *β*-, and *γ*-CD is displayed in Figure 3. For clockwise as well as anticlockwise orientation of hydroxyl groups in α-, *β*-, and *γ*-CD conformers, a similar trend of δ_H values has been observed. The hydroxyl functionalities in clockwise orientation lead to large δ_H values owing to strong hydrogen-bonded interactions. These are parallel to the ρ_{bcp} values given in Table 3. In *γ*-CD anticlockwise orientation (A1 and A4 conformers), the δ_H value is 4.62 and 4.68 ppm compared to 5.02 ppm for both the A2 and A3 conformers in which the hydroxyl groups are oriented in a clockwise fashion. Further, a correlation of the hydrogen-bond distances and the corresponding chemical shift is depicted in Figure 4. The $O_2H\cdots O_3'$ bond distances in the α-, *β*-, and *γ*-CD conformers are plotted as a function of δ_H of secondary hydroxyl protons (bottom rim) in Figure 4a which shows a remarkably linear correlation ($r^2 = 0.996$). Thus, an increase in the hydrogen-bond distance leads to a large deshielding of the proton; hence, a large downshift in the NMR spectrum can be predicted. For the clockwise hydrogen-bonding patterns in a bottom rim, that is, $O_3H\cdots O_2'$ interactions, a linear correlation with the chemical shift of a corresponding proton ($r^2 = 0.988$) can be seen from Figure 4b. From Figure 4, parts a and b, it may be concluded that the O_3H protons are more deshielded relative to those present in the anticlockwise inter-glucose hydrogen-bonded network (O_2H protons). These interactions fall into four distinct clusters, namely, I, II, III, and IV. Cluster I represents the protons from secondary hydroxyl groups participating in strong inter-glucose interactions as in "B" and "C" conformers, while Cluster II refers to conformers "A". Cluster III results from the intra-glucose interactions in "B" and "C" conformers, whereas these relatively weaker interactions in "A" conformers lead to lower δ_H values as in cluster IV in this figure. Thus, the hydrogen-bond distances in CD conformers can be correlated well to δ_H values in the NMR spectra.

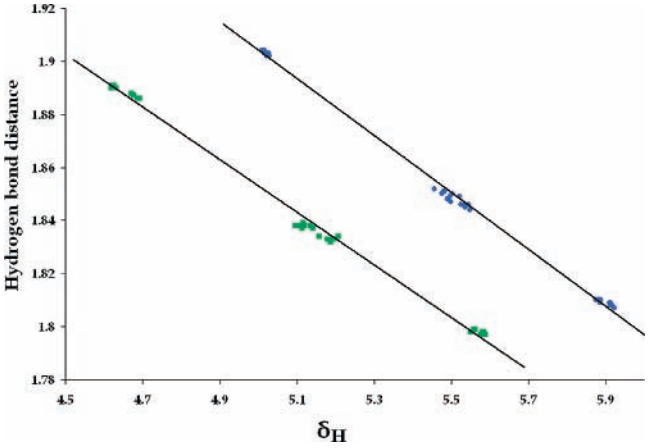

Figure 3. $O_6H\cdots O_6'$ distance vs δ_H in "A" conformers of α-, β-, and γ-CD. The green squares represent a hydroxyl proton in conformers with clockwise orientations of an −OH group in hydrogen bonds, whereas blue circles correspond to anticlockwise orientation.

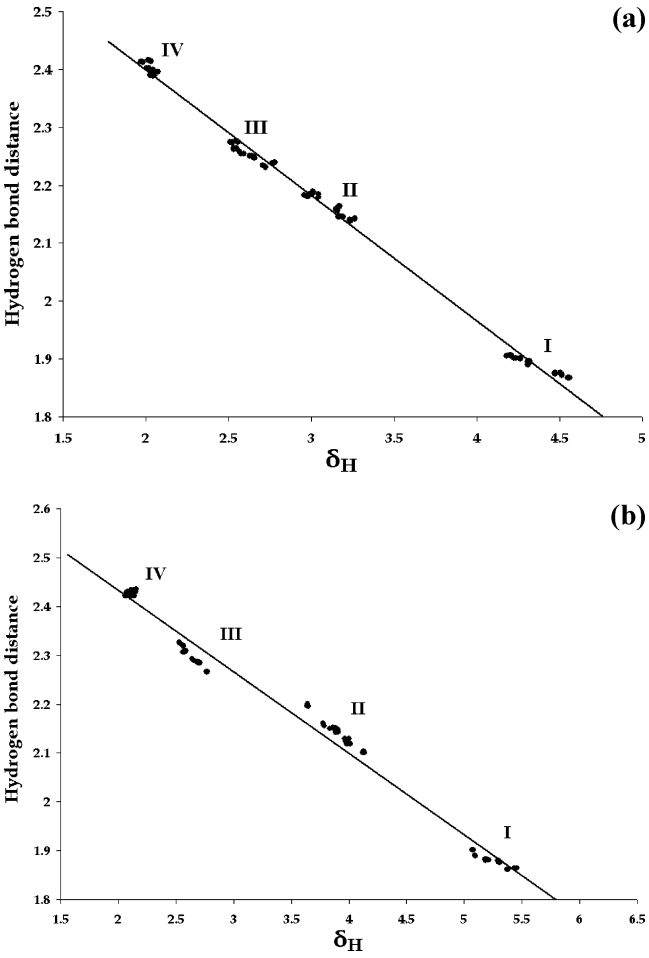

Figure 4. Hydrogen-bond distances in the bottom rim (secondary hydroxyl groups) of CD conformers plotted against the δ_H of the proton involved in hydrogen bonding. (a) $O_2H\cdots O_3'$ bond distance vs δ_H, (b) $O_3H\cdots O_2'$ bond distance vs δ_H.

It may further be noted here that the ρ_{bcp} value of a hydrogen bond provides a measure of its bond strength. A correlation of electron densities at the bcp (ρ_{bcp}) of the inter-glucose hydrogen bonds versus the calculated proton chemical shifts (δ_H) is depicted in Figure 5. It is gratifying to note that a linear plot (with a correlation coefficient of 0.991) is observed in the case of the $O_2H\cdots O_3'$ (shown in Figure 5a) and the $O_3H\cdots O_2'$ (Figure 5b) interactions as well. Thus the group exhibiting low ρ_{bcp} values in a plot represents the "A" type of conformers where the presence of relatively weak hydrogen-bonded interactions leads to a small downshift in the $\delta_H$value. On the other hand, stronger $O_3H\cdots O_2'$ interactions in "B"- and "C" types of conformers engender a further downshift of the proton. Thus the O_3H protons involved in the hydrogen-bonded interactions in the CD conformer show a relatively large downshift compared to the O_2H protons. This has also been observed in the measured NMR spectra.[36] Further, the chemical shift of protons from $C_6H\cdots O_5'$ interactions in the "A" type of conformers yields a good correlation with ρ_{bcp}.

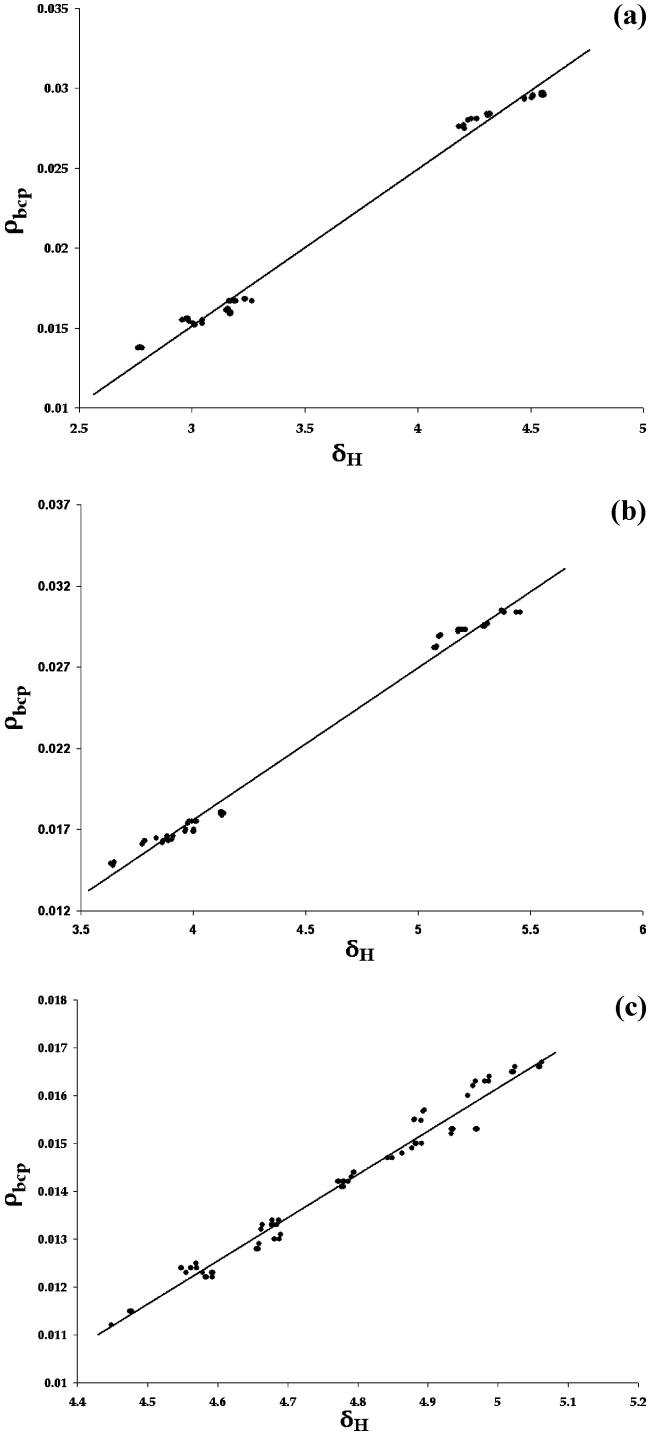

Figure 5. ρ_{bcp} of hydrogen bonds in the CD conformers plotted against δ_H of the proton involved in hydrogen bonding. Plot for hydrogen involved in (a) $O_2H\cdots O_3'$, (b) $O_3H\cdots O_2'$, and (c) $C_6H\cdots O_5'$ interactions.

TABLE 5: Dipole Moments, μ, (in Debye) in CD Conformers

	α-CD	β-CD	γ-CD
A1	2.0	1.3	0.5
A2	1.6	1.2	0.7
A3	2.9	2.5	2.0
A4	0.7	−0.1[a]	−0.8[a]
B2	6.5	7.3	8.1
B3	7.5	8.3	9.2
C1	7.1	7.7	8.4
C4	5.7	6.4	7.0

[a] The negative sign here represents the reversal of the net dipole moment vector.

B3LYP/6-31G(d,p)-calculated dipole moments of α-, β-, and γ-CD conformers are shown in Table 5. Dipole moments of CD conformers are governed primarily by hydrogen-bonding patterns in the top rim (primary hydroxyl groups). The dipole moment of the "A" type of conformers decreases steadily with increasing number of glucose units as seen from α-CD to β-CD to γ-CD, unlike for the "B" and "C" types of conformers. Figure 1S, see Supporting Information, depicts the resultant (net) dipole moment vector of α-, β-, and γ-CD conformers. It can be observed that for "B" and "C" types of conformers the dipole moment increases steadily on going from α-CD to γ-CD, which is partly attributed to the number of secondary OH groups in the bottom rim. This engenders a large resultant dipole moment vector by addition of bond dipole moments of these hydroxyl groups. Further delocalization of electron-rich regions to a larger extent in the top rim results in a higher dipole moment for the CD conformer. On the other hand, for the "A" type of conformers, facilitating the $O_6H\cdots O_6'$ interactions between primary hydroxyl groups leads to localized electron-rich regions which results in a cancellation of bond moments and hence a decrease in the resultant molecular dipole moment can be noticed. This explains why A1−A4 conformers yield smaller dipole moments. It should further be remarked here that the resultant dipole moment vector is directed from the center of the top rim to the bottom one in all these CD conformers except in case of the A4 conformer of β- and γ-CD, where it points in the opposite direction.

In order to understand the influence of solvent on relative stabilization of CD conformers, the self-consistent reaction field (SCRF) calculations have been carried out. The polar (ranging from water to ethanol or acetone) as well as nonpolar solvents (viz., tetrahydrofuran (THF), cyclohexanol, and heptane) were considered. Relative stabilization energies (in kJ mol^{-1}) thus obtained are reported in Table 6. The polar solvents have a profound influence on the relative stabilization of "B" and "C" conformers, which gets lowered in energy in the presence of these solvents. It may further be remarked here that the effect from the water or acetonitrile is more pronounced in the case of C1 and C4 conformers of β- or γ-CD, which turns out to be 38.0 kJ mol^{-1} lower in energy than A1 (which was the lowest-energy conformer in the gas phase). In the case of the nonpolar solvents, the energy rank order of the relative stabilization energies turns out to be the same as that predicted for the gas phase.

The effect of solvents (viz., water, ethanol, and heptane, representing high, medium, and less (non-) polar solvents, respectively) on NMR chemical shifts of hydroxyl protons in CD conformers have been investigated. The chemical shifts calculated in the presence of solvent using TMS in respective solvents as a reference are displayed in Table 7. As may be noticed, δ_H for the proton in hydrogen-bonded interactions is nearly unchanged by solvation compared to those predicted from the gas-phase calculations. For example, chemical shifts of H_3 protons in A1 turn out to be 3.8 ppm in the gas phase as well as in solvents. On the contrary, the protons which do not participate in the hydrogen-bonded interactions show a downshift (largest, i.e., ∼1 ppm for primary hydroxyl proton from the top rim in "C" type conformers) in water as compared to gas phase, and this downshift amounts to 0.8 and 0.6 ppm in ethanol and heptane, respectively. Thus it may be conjectured that the already deshielded proton due to hydrogen-bonded

TABLE 6: Relative Stabilization Energies (in kJ mol^{-1}) of α-, β-, and γ-CD Conformers in Different Solvents

	water	acetonitrile	methanol	ethanol	acetone	THF	cyclohexane	heptane
				α-CD				
A1	0.0	0.0	0.0	0.0	0.0	0.0	0.0	0.0
A2	−13.2	−12.3	−11.2	−12.0	−11.8	−8.6	−2.5	−10.7
A3	−0.7	−3.3	−2.5	−3.1	−2.8	−2.2	−0.4	−6.5
A4	−10.9	−8.1	−7.3	−7.8	−7.9	−4.4	−1.2	−12.9
B2	35.7	34.7	39.1	36.4	47.3	55.4	71.2	68.2
B3	32.8	35.3	36.1	36.9	47.6	58.0	73.2	67.6
C1	5.4	6.0	8.1	8.3	20.9	37.1	66.6	62.8
C4	2.4	7.0	9.2	11.6	24.0	35.8	62.9	59.9
				β-CD				
A1	0.0	0.0	0.0	0.0	0.0	0.0	0.0	0.0
A2	−16.1	−3.3	−2.7	−2.9	−2.7	6.3	3.8	−0.1
A3	0.2	4.2	4.4	4.3	4.8	10.8	6.3	7.3
A4	−17.9	−8.8	−8.0	−8.6	−8.7	8.2	4.3	−0.1
B2	23.6	29.0	30.4	29.9	28.4	48.2	61.0	57.1
B3	7.9	25.8	27.3	27.5	29.7	47.7	52.2	62.8
C1	−19.6	−6.9	−9.2	−4.0	0.2	25.5	54.4	
C4	−16.0	−2.6	−3.5	0.2	1.0	26.4	53.7	52.9
				γ-CD				
A1	0.0	0.0	0.0	0.0	0.0	0.0	0.0	0.0
A2	4.4	16.9	9.3	9.8	8.4	10.1	15.7	16.3
A3	16.9		14.7	14.3	14.6	14.1	16.5	17.3
A4	−9.7	−9.6	−4.8	−4.3	−5.1	−3.0	1.6	0.8
B2	13.5	10.2	17.0	17.1	14.4	26.5	51.6	47.4
B3	10.8	11.3	14.6	14.7	14.5	21.5	57.0	45.9
C1	−38.0	−30.6	−29.5	−22.6	−20.2	−1.3	37.4	67.6
C4	−32.5	−27.8	−21.7	−19.3	−17.5	−0.2	41.0	38.2

TABLE 7: NMR Chemical Shifts of Hydroxyl Protons of α-CD Conformers in Different Solvents

		gas phase	water	ethanol	THF
A1	H_2	2.1	2.9	2.8	2.7
	H_3	3.8	3.8	3.8	3.8
	H_6	5.6	5.4	5.4	5.5
A2	H_2	2.8	2.8	2.8	2.8
	H_3	2.1	2.9	2.8	2.7
	H_6	5.9	5.8	5.8	5.8
A3	H_2	2.0	2.9	2.8	2.6
	H_3	3.6	3.6	3.6	3.6
	H_6	5.9	5.8	5.8	5.8
A4	H_2	3.0	3.0	3.0	3.0
	H_3	2.1	3.0	2.8	2.7
	H_6	5.6	5.4	5.5	5.5
B2	H_2	4.3	4.4	4.4	4.4
	H_3	2.6	3.4	3.2	3.1
	H_6	2.9	3.2	3.2	3.1
B3	H_2	2.6	3.3	3.2	3.1
	H_3	5.1	5.1	5.1	5.1
	H_6	2.9	3.2	3.1	3.0
C1	H_2	2.5	3.3	3.2	3.1
	H_3	5.1	5.1	5.1	5.1
	H_6	1.3	2.2	2.1	1.9
C4	H_2	4.2	4.3	4.3	4.3
	H_3	2.5	3.3	3.2	3.1
	H_6	1.3	2.3	2.1	1.9

interactions has not further been influenced significantly by the solute−solvent interactions.

Conclusions

Strength of hydrogen-bonded interactions in different α-, β-, and γ-CD conformers have been analyzed using the molecular electron density topography and calculated NMR chemical shifts. The following conclusions may be drawn. (i) The $O_3-H\cdots O_2'$ hydrogen-bonded interactions render large stability to α-, β-, and γ-CD conformers compared to the $O_2-H\cdots O_3'$ interactions. (ii) The strength of hydrogen-bonded interactions involving primary hydroxyl groups follows the rank order α-CD > β-CD > γ-CD, while the reverse trend has been noticed for the secondary hydroxyl groups. These inferences are supported by MED topography and calculated NMR chemical shifts. (iii) The hydrogen-bond distance can be correlated to δ_H values of primary hydroxyl groups and exhibits a linear correlation. For secondary hydroxyl groups, a linear plot showing four distinct clusters is obtained. These results can be rationalized on the basis of the strength of hydrogen-bonded interactions. (iv) Polar solvents have a profound influence on the relative stabilization of C1 and C4 conformers of β- and γ-CD which turn out to be lower-energy conformers unlike in the gas phase. (v) Chemical shifts of protons involved in hydrogen-bonded interactions are nearly insensitive to solvation. On the other hand, the downshift of protons not participating in such interactions increases steadily with the polarity of the solvent.

Acknowledgment. S.P.G. is grateful to the University Grants Commission (UGC), New Delhi, India (Research Project F30-72/2004(SR)) and to the University of Pune for disbursing the research grant under the potential excellence (UPE) scheme. R.V.P. and K.A.J. thank the Council of Scientific and Industrial Research (CSIR) for senior research fellowships. The authors thank the center for network computing, University of Pune, for providing computational facilities.

Supporting Information Available: Cartesian coordinates of atoms in the α-, β-, and γ-CD conformers from the B3LYP/6-31G(d) optimizations, Figure 1S showing resultant dipole moment vector in these CD conformers. This material is available free of charge via the Internet at http://pubs.acs.org.

References and Notes

(1) Szejtli, J. *Chem. Rev.* **1998**, *98*, 1743.
(2) Loftsson, T.; Brewster, M. E. *J. Pharm. Sci.* **1996**, *85*, 1017.
(3) Thompson, D. O. *CRC Crit. Rev. Ther. Drug Carrier Syst.* **1997**, *14*, 1.
(4) Uekama, K.; Hirayama, F.; Irie, T. *Chem. Rev.* **1998**, *98*, 2045.
(5) Connors, K. A. *Chem. Rev.* **1997**, *97*, 1325.
(6) Uekama, K. *J. Inclusion Phenom. Macrocycl. Chem.* **2002**, *44*, 3.
(7) Kano, K.; Hasegawa, H. *J. Inclusion Phenom. Macrocycl. Chem.* **2001**, *41*, 41.
(8) Buschmann, H. J.; Knittel, D.; Schollmeyer, E. *J. Inclusion Phenom. Macrocycl. Chem.* **2001**, *40*, 169.
(9) Monti, S.; Sortino, S. *Chem. Soc. Rev.* **2002**, *31*, 287.
(10) Harada, A. *Acc. Chem. Res.* **2001**, *34*, 456.
(11) Guillaume, Y. C.; Guinchard, C. *J. Phys. Chem. B* **1997**, *101*, 8390.
(12) Abreu, A. R.; Costa, I.; Rosa, C.; Ferreira, L. M.; Lourenço, A.; Santos, P. P. *Tetrahedron* **2005**, *61*, 11986.
(13) Wenz, G. *Angew. Chem., Int. Ed. Engl.* **1994**, *33*, 803.
(14) Saenger, W.; Steiner, T. *Acta Crystallogr., Sect. A* **1998**, *54*, 798.
(15) Schneider, H.; Hacket, F.; Rüdiger, V. *Chem. Rev.* **1998**, *98*, 1755.
(16) Onda, M.; Yamamoto, Y.; Inoue, Y.; Chûjô, R. *Bull. Chem. Soc. Jpn.* **1988**, *61*, 4015.
(17) Casu, B.; Reggioni, M.; Gallo, G. G.; Vigevani, A. *Chem. Soc.* (*London*) **1968**, Spec. Publ. No. 23, 217.
(18) Harata, K. *Bull. Chem. Soc. Jpn.* **1987**, *60*, 2363.
(19) Fraser, R. R.; Kaufman, M.; Morand, P.; Govil, G. *Can. J. Chem.* **1969**, *47*, 403.
(20) Lipkowitz, K. B. *J. Org. Chem.* **1991**, *56*, 6357.
(21) Dobado, J. A.; Benkadour, N.; Melchor, S.; Portal, D. *J. Mol. Struct.* (Theochem) **2004**, *672*, 127.
(22) Pinjari, R. V.; Joshi, K. A.; Gejji, S. P. *J. Phys. Chem. A* **2006**, *110*, 13073.
(23) Avakyan, V. G.; Nazarov, V. B.; Voronezheva, N. I. *Russ. J. Phys. Chem.* **2005**, *79*, S18.
(24) Snor, W.; Liedl, E.; Weiss-Greiler, P.; Karpfen, A.; Viernstein, H.; Wolschann, P. *Chem. Phys. Lett.* **2007**, *441*, 159.
(25) Nascimento, C. S., Jr.; Dos Santos, H. F.; De Almeida, W. B. *Chem. Phys. Lett.* **2004**, *397*, 422.
(26) Becke, A. D. *J. Chem. Phys.* **1993**, *98*, 5648.
(27) Lee, C.; Yang, W.; Parr, R. G. *Phys. Rev. B* **1988**, *37*, 785.
(28) Frisch, M. J.; Trucks, G. W.; Schlegel, H. B.; Scuseria, G. E.; Robb, M. A.; Cheeseman, J. R.; Montgomery, J. A., Jr.; Vreven, T.; Kudin, K. N.; Burant, J. C.; Millam, J. M.; Iyengar, S. S.; Tomasi, J.; Barone, V.; Mennucci, B.; Cossi, M.; Scalmani, G.; Rega, N.; Petersson, G. A.; Nakatsuji, H.; Hada, M.; Ehara, M.; Toyota, K.; Fukuda, R.; Hasegawa, J.; Ishida, M.; Nakajima, T.; Honda, Y.; Kitao, O.; Nakai, H.; Klene, M.; Li, X.; Knox, J. E.; Hratchian, H. P.; Cross, J. B.; Bakken, V.; Adamo, C.; Jaramillo, J.; Gomperts, R.; Stratmann, R. E.; Yazyev, O.; Austin, A. J.; Cammi, R.; Pomelli, C.; Ochterski, J. W.; Ayala, P. Y.; Morokuma, K.; Voth, G. A.; Salvador, P.; Dannenberg, J. J.; Zakrzewski, V. G.; Dapprich, S.; Daniels, A. D.; Strain, M. C.; Farkas, O.; Malick, D. K.; Rabuck, A. D.; Raghavachari, K.; Foresman, J. B.; Ortiz, J. V.; Cui, Q.; Baboul, A. G.; Clifford, S.; Cioslowski, J.; Stefanov, B. B.; Liu, G.; Liashenko, A.; Piskorz, P.; Komaromi, I.; Martin, R. L.; Fox, D. J.; Keith, T.; Al-Laham, M. A.; Peng, C. Y.; Nanayakkara, A.; Challacombe, M.; Gill, P. M. W.; Johnson, B.; Chen, W.; Wong, M. W.; Gonzalez, C.; Pople, J. A. *Gaussian 03*, Revision C.02; Gaussian, Inc.: Wallingford, CT, 2004.
(29) Wolinski, K.; Hilton, J. F.; Pulay, P. *J. Am. Chem. Soc.* **1990**, *112*, 8251.
(30) Bader, R. F. W. In *Atoms in Molecules: A Quantum Theory*; Oxford University Press, Clarendon: U.K., 1990.
(31) Koch, U.; Popelier, P. L. A. *J. Phys. Chem.* **1995**, *99*, 9747.
(32) Popelier, P. L. A. *J. Phys. Chem. A* **1998**, *102*, 1873.
(33) Balanarayan, P.; Gadre, S. R. *J. Chem. Phys.* **2003**, *119*, 5037.
(34) Limaye, A. C.; Gadre, S. R. *Curr. Sci.* **2001**, *80*, 1298.
(35) Miertus, S.; Scrocco, E.; Tomasi, J. *Chem. Phys.* **1981**, *55*, 117.
(36) Bekiroglu, S.; Kenne, L.; Sandstrom, C. *J. Org. Chem.* **2003**, *68*, 1671.